800 MHz cavity design update and new damping scheme (for Z, W, H booster)

Shahnam Gorgi Zadeh

Study goals

Cryomodule length reduction

- **Coaxial Extractors**: were placed between cavities to extract HOM power from broadband impedance and damp trapped modes in interconnecting beam pipes
- **Length constraint**: Coupler removal to save at least 795 mm per cryomodule (3 × 265 mm)
- Evaluate effects on **HOM impedance** and update design if needed

Beam impedance constraint for booster cavities in reverse phase operation (RPO)

- The same number of cavities will be used for the Z, W and H booster system in the RPO
- Evaluate the beam stability limit for different working points

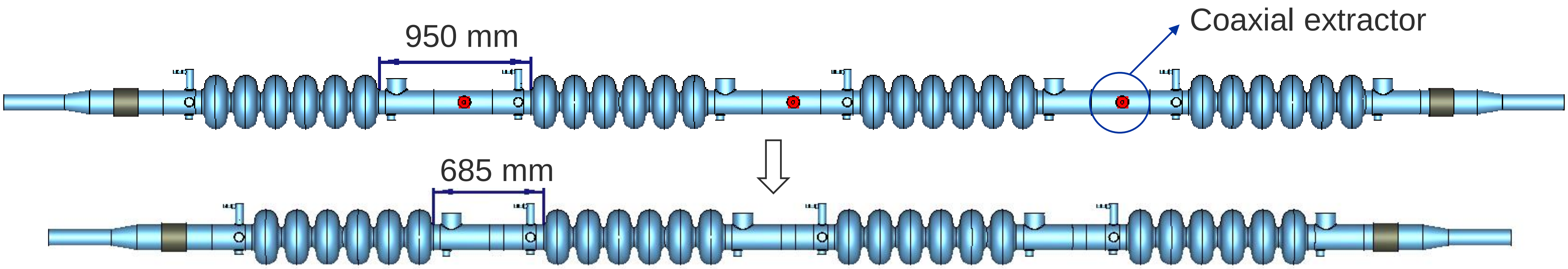

$t\bar{t}$ and booster stability parameters

- Low energy and long damping time at injection leads to a low beam instability impedance limit for the booster cavities
- A 100-turn feedback for the transverse plane, and a factor of three energy loss per turn from wigglers considered in the longitudinal plane impedance

Running mode	Z-booster	W-booster	Higgs-booster	ttbar-booster	ttbar-collider
Momentum compaction (α_c)	7.12e-6				7.52e-6
Current (I_0) [mA]	14.8	11.8	2.01	0.30	0.0049×2
Injection					
Injection energy (E_0) [GeV]	20	20	20	20	
Long. Damping time (τ_z) [s]	4.52	4.52	4.52	4.52	
Sync. tune at injection	0.0262	0.0262	0.0262	0.0262	
$Z_{\parallel}^{th}$ [MΩ] with SR	$2.2/f$ [GHz]	$2.8/f$ [GHz]	$16.2/f$ [GHz]	$108.5/f$ [GHz]	
$Z_{\perp}^{th}$ [MΩ/m] with SR	1.8	2.3	13.3	89.2	
$Z_{\parallel}^{th}$ [MΩ] with $\tau_z = 1.51\ s$	**$6.6/f$ [GHz]**	**$8.4/f$ [GHz]**	**$48.6/f$ [GHz]**	**$326/f$ [GHz]**	
$Z_{\perp}^{th}$ [MΩ/m] with 100 turns FB	**545**	**683**	**4012**	**26879**	
Extraction					
Extraction energy [GeV]	45.6	80	120	182.5	182.5
Long. Damping time at extraction [s]	0.382	0.0707	0.0209	0.00595	0.0059
Sync. tune at extraction	0.0163	0.0269	0.0458	0.0795	0.0881
$Z_{\parallel}^{th}$ [MΩ]	$36.9/f$ [GHz]	$724.6/f$ [GHz]	$36750/f$ [GHz]	$2283189/f$ [GHz]	$74372/f$ [GHz]
$Z_{\perp}^{th}$ [MΩ/m]	48.8	580	17277	618363	19197

$$Z_{\parallel}^{\mathrm{th}} = \frac{2(E_0/q_e)\nu_s}{N_{\mathrm{cav}} f I_0 \alpha_c \tau_z},$$

$$Z_{\perp}^{\mathrm{th}} = \frac{2(E_0/q_e)}{N_{\mathrm{cav}} f_{\mathrm{rev}} I_0 \beta_{xy} \tau_{xy}}$$

- Transversal damping time $(\tau_{xy}) = 2\times$ longitudinal damping time (τ_z)
- $\beta_{xy} = 50$ m for all working points, $f_{rev} = 3307$ Hz, N_{cav} is assumed 1 (a normalization to the number of cavities is needed)

Parameters affecting total impedance

- **Cavity shape:**
  - The damping of the mode at 2.368 GHz can be improved by modifying the end-cell (details in the appendix).
  - The new end-cell traps a dipole mode in the cavity at 1.89 GHz
- **HOM coupler design**
  - Inner coax diameter of the coupler increased for better robustness and simpler inner cooling
  - The lower part of the coupler modified to decrease B_{pk} on the coupler from $20\,\mathrm{mT}$ to $14\,\mathrm{mT}$ at $E_{\mathrm{acc}} = 20\,\mathrm{MV/m}$ (as a reference it is $90.6\,\mathrm{mT}$ in DQW cavity at $V_{\perp} = 3.4\,\mathrm{MV/m}$)
- **Frequency spread of HOMs**
  - Manufacturing errors cause frequency shifts in HOMs, resulting in varying HOM frequencies across cavities and spreading impedance over different frequencies

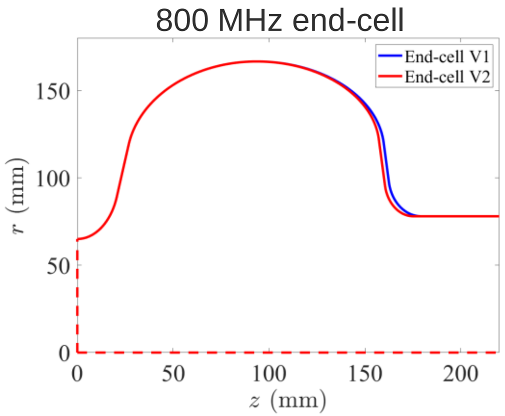

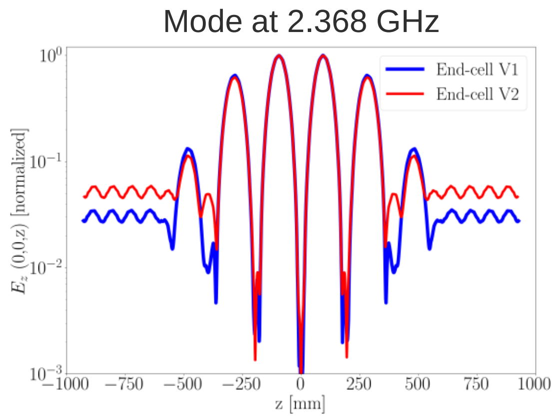

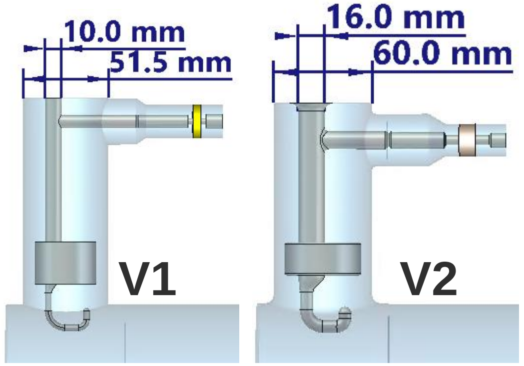

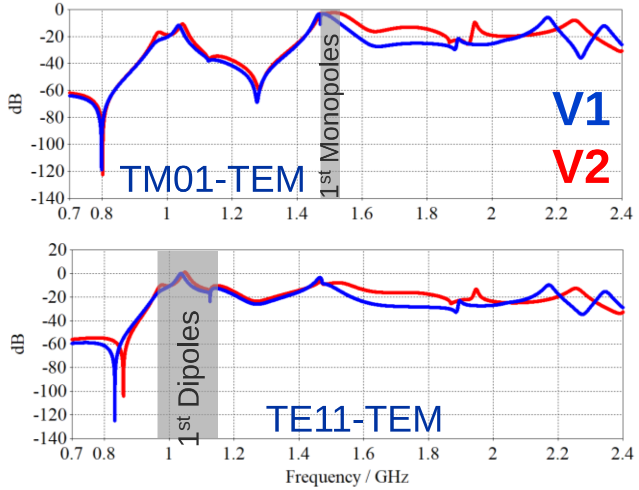

Frequency spread coefficient

- If impedance for mode m modelled by $Z_{\parallel,m}(f) \approx \frac{1}{2}\frac{R/Q_{\parallel,m}\cdot Q_m}{1+jQ_m(f/f_m - f_m/f)}$ → $\boldsymbol{c} = \frac{\sum_{n=1}^{N_{\text{cav}}} Z_{\parallel,n,m}}{N_{\text{cav}} Z_{\parallel,1,m}}$: the ratio of the total impedance of N_{cav} cavities, each with a perturbed shape, to the impedance of N_{cav} cavities with identical shape

$f_n = 2$ GHz		$N_{\text{cav}} = 1$	$N_{\text{cav}} = 4$	$N_{\text{cav}} = 10$	$N_{\text{cav}} = 50$	$N_{\text{cav}} = 100$	$N_{\text{cav}} = 400$
$\sigma(f_n) = 10$ kHz	$Q_n = 1e3$	1	1	1	1	1	1
	$Q_n = 1e4$	1	1	1	1	1	0.99
	$Q_n = 1e5$	1	0.85	0.81	0.79	0.79	0.79
	$Q_n = 1e6$	1	0.51	0.35	0.29	0.26	0.25
$\sigma(f_n) = 100$ kHz	$Q_n = 1e3$	1	1	1	1	1	1
	$Q_n = 1e4$	1	0.85	0.82	0.80	0.79	0.78
	$Q_n = 1e5$	1	0.47	0.38	0.28	0.26	0.24
	$Q_n = 1e6$	1	0.31	0.18	0.087	0.065	0.05
$\sigma(f_n) = 1000$ kHz	$Q_n = 1e3$	1	0.86	0.82	0.79	0.80	0.79
	$Q_n = 1e4$	1	0.47	0.36	0.29	0.26	0.25
	$Q_n = 1e5$	1	0.29	0.16	0.08	0.065	0.05
	$Q_n = 1e6$	1	0.25	0.11	0.039	0.025	0.014

Perturbation analysis

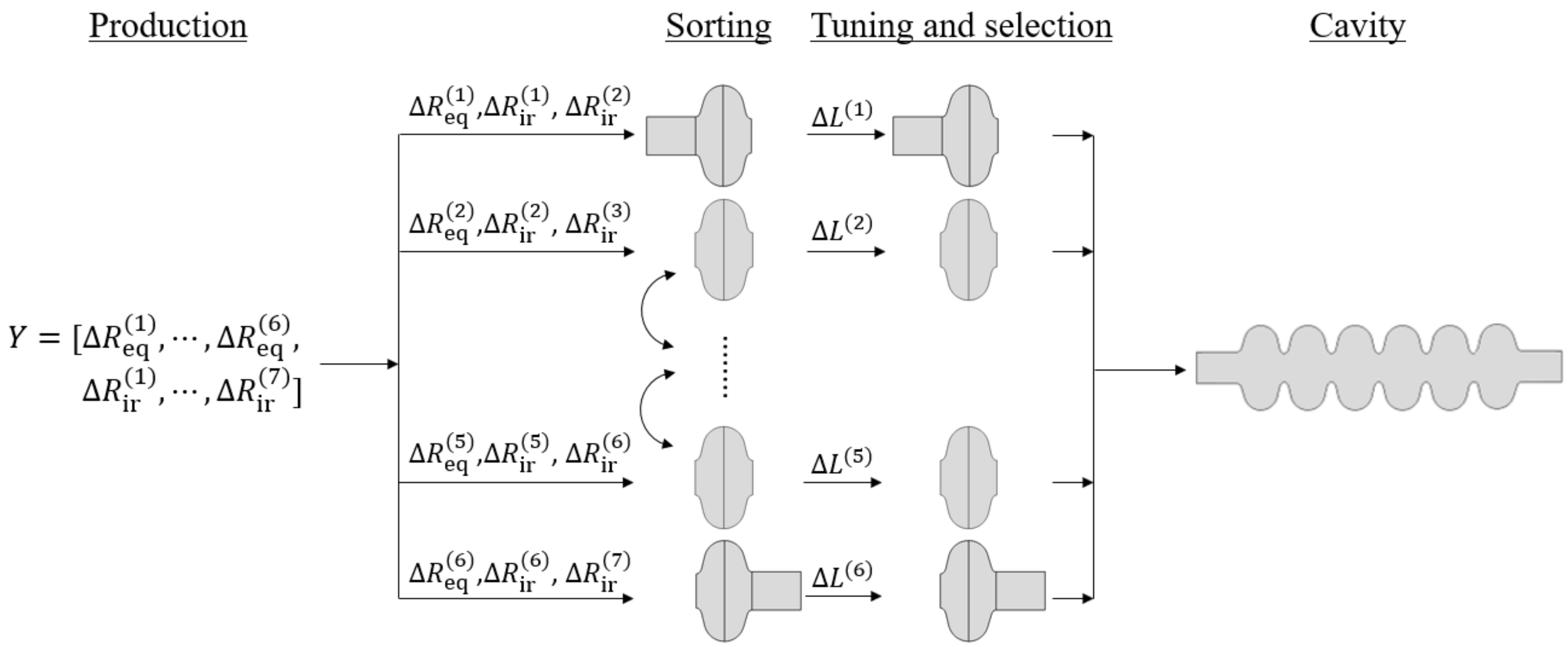

- A **perturbation** applied to R_{ir} and R_{eq} with a standard deviation of 0.1 mm clamped at [-0.3 mm, 0.3 mm]. The length of each cell is then changed to tune the cells' frequency to 801.58 MHz.
- **Sorting before tuning**: the mid-cell with average frequency is installed at the last position (position 5), the remaining mid-cells are installed in order of decreasing frequency

J. Corno, et al.Uncertainty modeling and analysis of the European X-ray free electron laser cavities manufacturing process, 2020

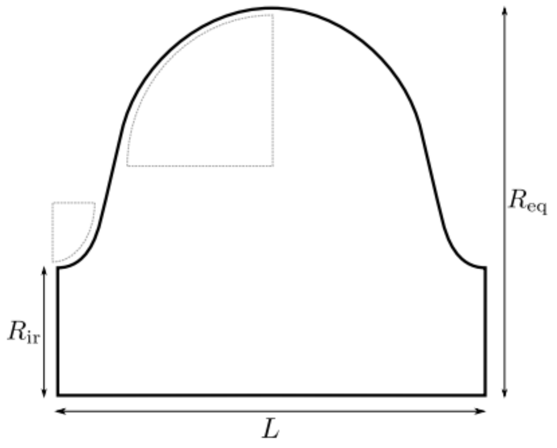

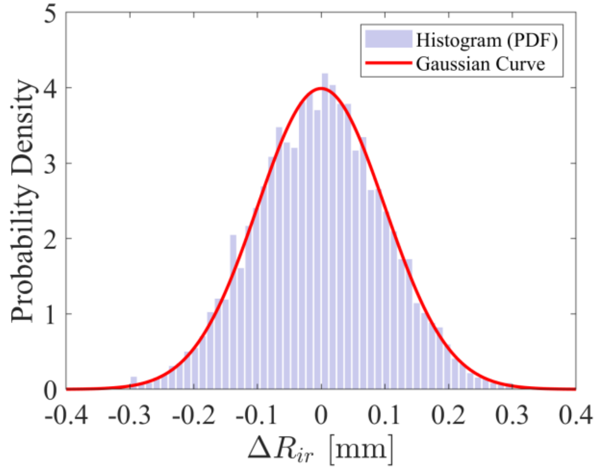

FM passband sensitivity to perturbations

- Perturbations applied without cell sorting and the frequency of FM passband and three HOMs with large longitudinal impedance is calculated

- The impedances are normalized to 88 cavities required for Z, W, and H booster in reverse phase operation and compared with the impedance limit for the Z booster with $\tau_Z = 1.51\ s$ → m4 has the highest impedance and by more than a factor 2 is below the stability limit

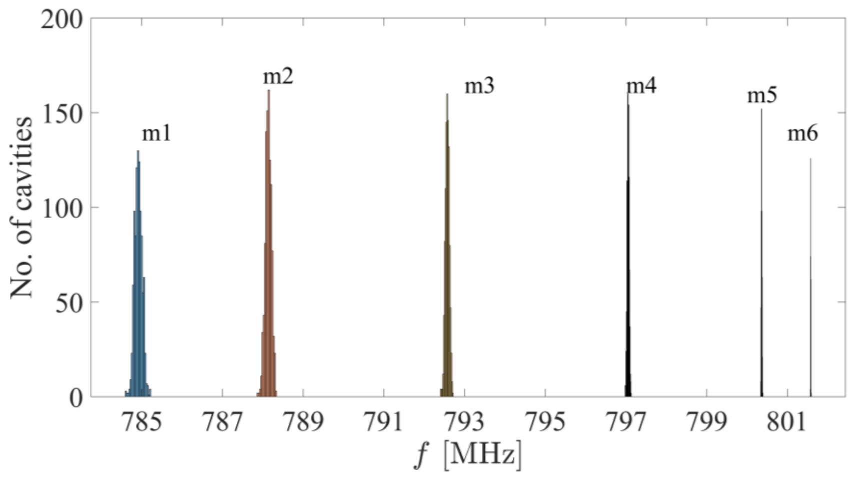

	m1	m2	m3	m4	m5	m6=FM	HM1	HM2	HM3
$\bar{f}$ [MHz]	784.914	788.136	792.572	797.052	800.363	801.581	1497.3	2368.8	2862.0
Std (f) [kHz]	93.2	73.6	48.7	24.0	8.9	3.5	787	1826	912
$\overline{R/Q}$ [Ω]	0.0089	0.134	0.035	0.45	0.1	629.2	113.9	24.2	22.8
Q_{ext}	3.3e7	8.6e6	4.3e6	2.9e6	2.3e6	4.3e6	-	-	-
Q_{ext}	9.5e7	2.4e7	1.1e7	7.1e6	5.7e6	1.1e7	-	-	-

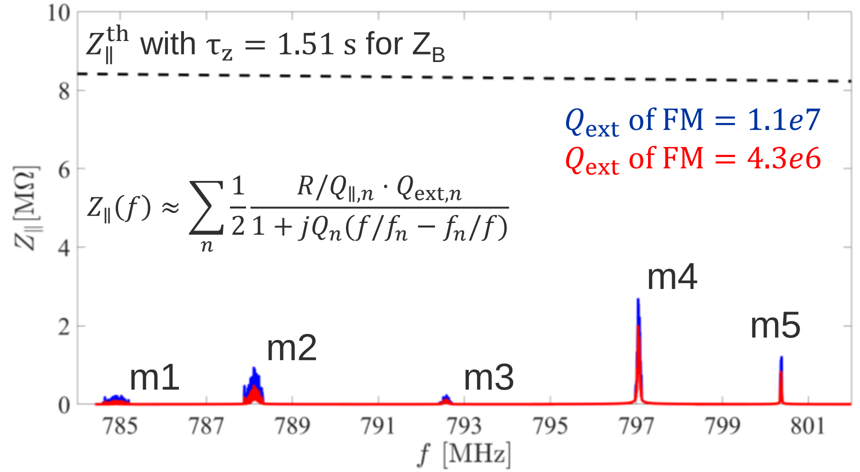

- $\bar{f}$ =mean value of frequency, and Std (f)=standard deviation of frequency
- HM is the higher order modes at different passbands with largest longitudinal R/Q
- 1000 samples were taken

HOM sensitivity to perturbations

- Perturbations applied to 250 cavities; longitudinal impedances added and normalized to 88 cavities
- Cell sorting reduces the chance of trapped modes and end-cell V2 has lower longitudinal impedance
- Q_{ext} arising from open boundary conditions of a single cavity is idealistic because the mode propagates into the adjacent cavity rather than being absorbed by a damper. A coaxial coupler tuned to 2.368 GHz is needed to damp this mode. However, its damping may be weaker than with open BC, i.e. the impedance of this mode in a cryomodule could be higher.

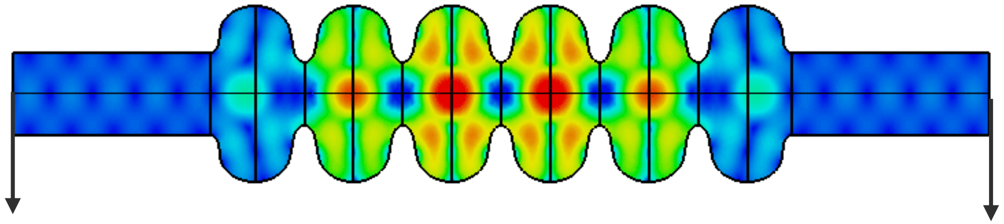

Open BC

Open BC

Superposition of $Z_{\parallel}$ of 88 perturbed cavities

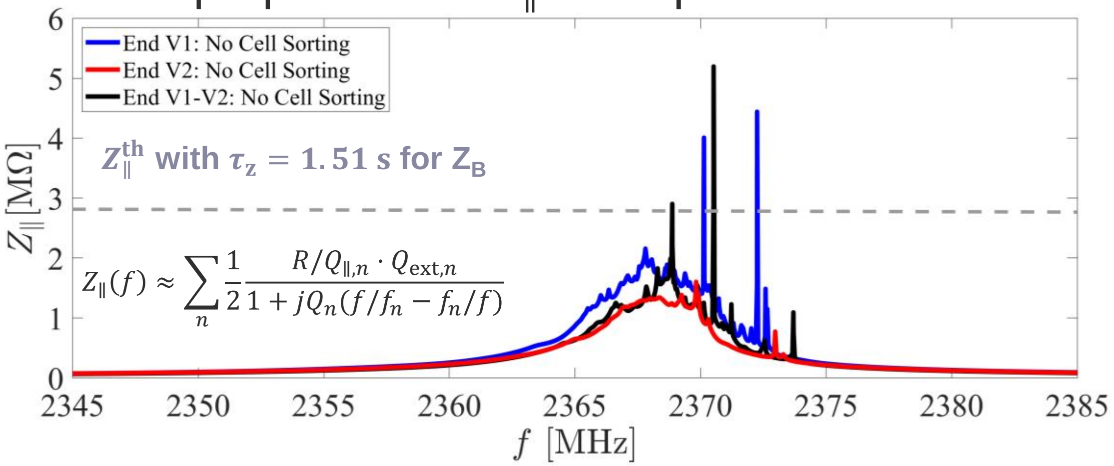

Cell sorting after perturbation

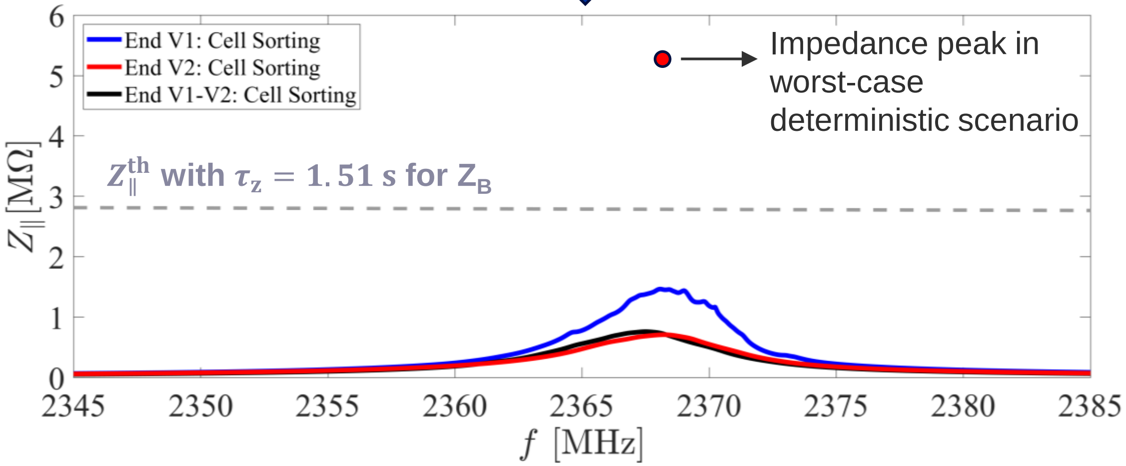

Impedance without perturbation in a module

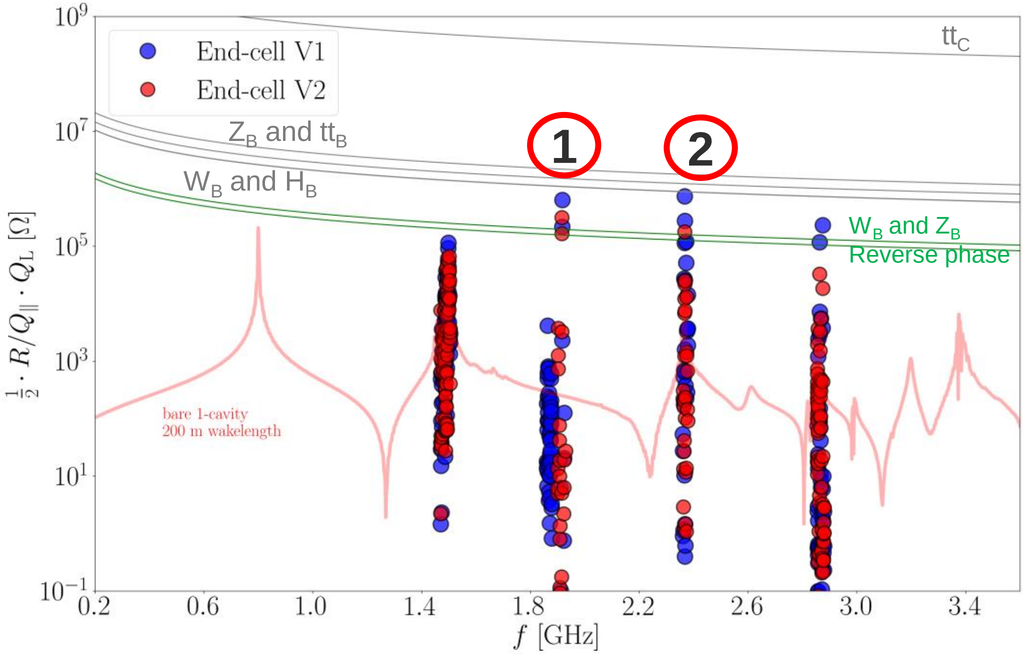

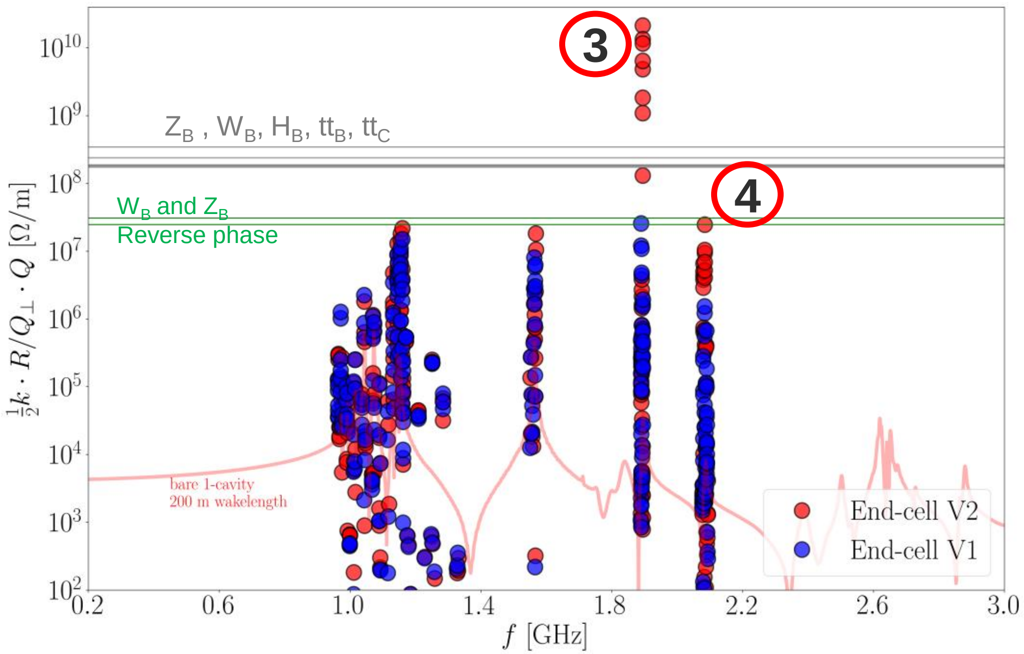

1

$f = 1.916$ GHz, $R/Q = 1.4$ Ω, $Q_L = 4.5e5, c = 0.08$

2

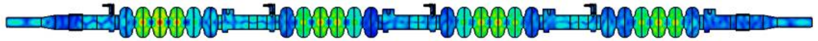

$f = 2.367$ GHz, $R/Q = 73.6$ Ω, $Q_L = 4.9e3, c = 0.33$

3

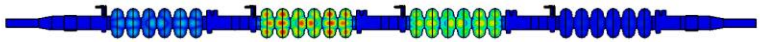

$f = 1.894$ GHz, $R/Q_{\perp} = 0.8$ Ω, $Q_L = 1.4e9$

4

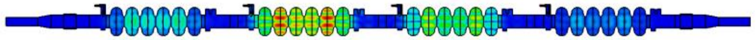

$f = 2.084$ GHz, $R/Q_{\perp} = 0.29$ Ω, $Q_L = 3.9e6$

End-cell V2 improves $Z_{\parallel}$ but worsens $Z_{\perp}$ peak. Asymmetric end-cells can provide a compromise between the two → next slide

$Z_{\parallel}$ of asymmetric end-cells with 4 DQW couplers

- Two additional DQW couplers, tuned for better damping of the 2.368 GHz mode, were added to the empty ports

- The impedance peak remains slightly above the limit; however, considering the frequency spread between cavities ($c = 0.12$ for this mode), stability is expected to be maintained in RPO

1 $\boldsymbol{f = 2.3676\ \mathrm{GHz}, R/Q = 18.0\ \Omega, Q_L = 22.4e3, c = 0.12}$

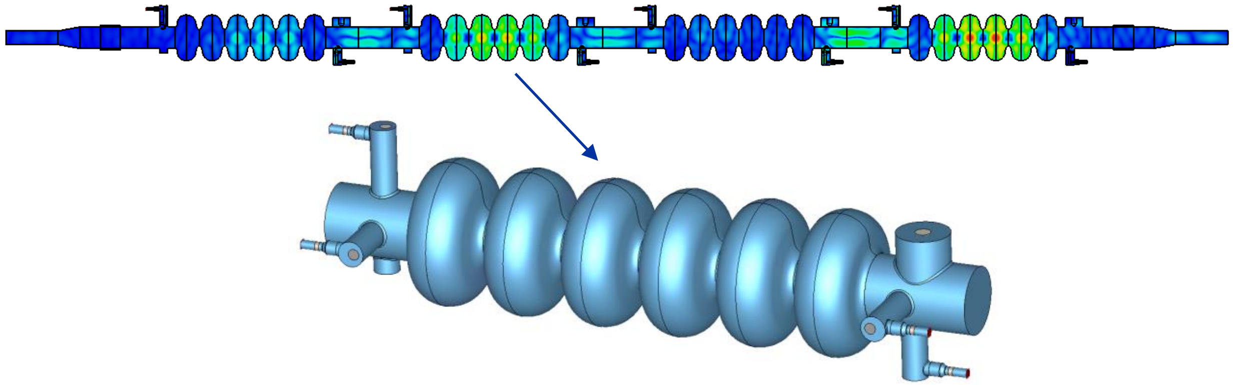

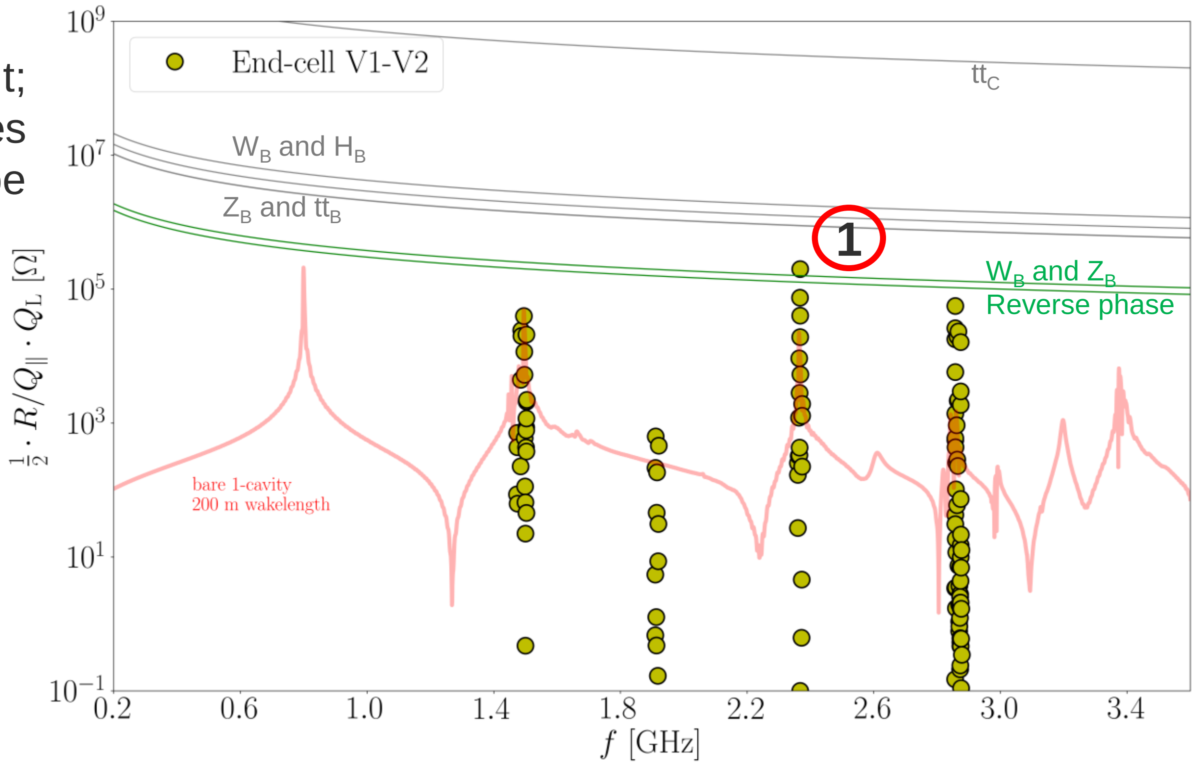

$Z_\perp$ of asymmetric end-cells with 4 DQW couplers

- For transverse impedance we are also close to the stability limit, but the frequency spread between cavities can improve the stability limit by at least a factor five

1 $f = 1.154\ \text{GHz}, R/Q_\perp = 54.0\ \Omega, Q_L = 2.2e4$ → $c(\sigma = 0.5\ \text{MHz}) = 0.18$, $c(\sigma = 1.0\ \text{MHz}) = 0.12$

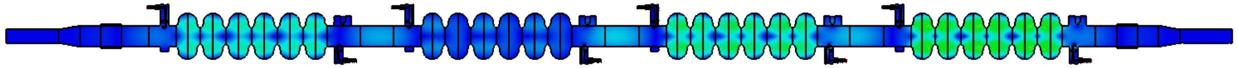

2 $f = 1.574\ \text{GHz}, R/Q_\perp = 53.5\ \Omega, Q_L = 3.6e4$ → $c(\sigma = 0.5\ \text{MHz}) = 0.17$, $c(\sigma = 1.0\ \text{MHz}) = 0.11$

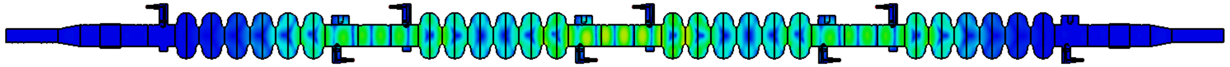

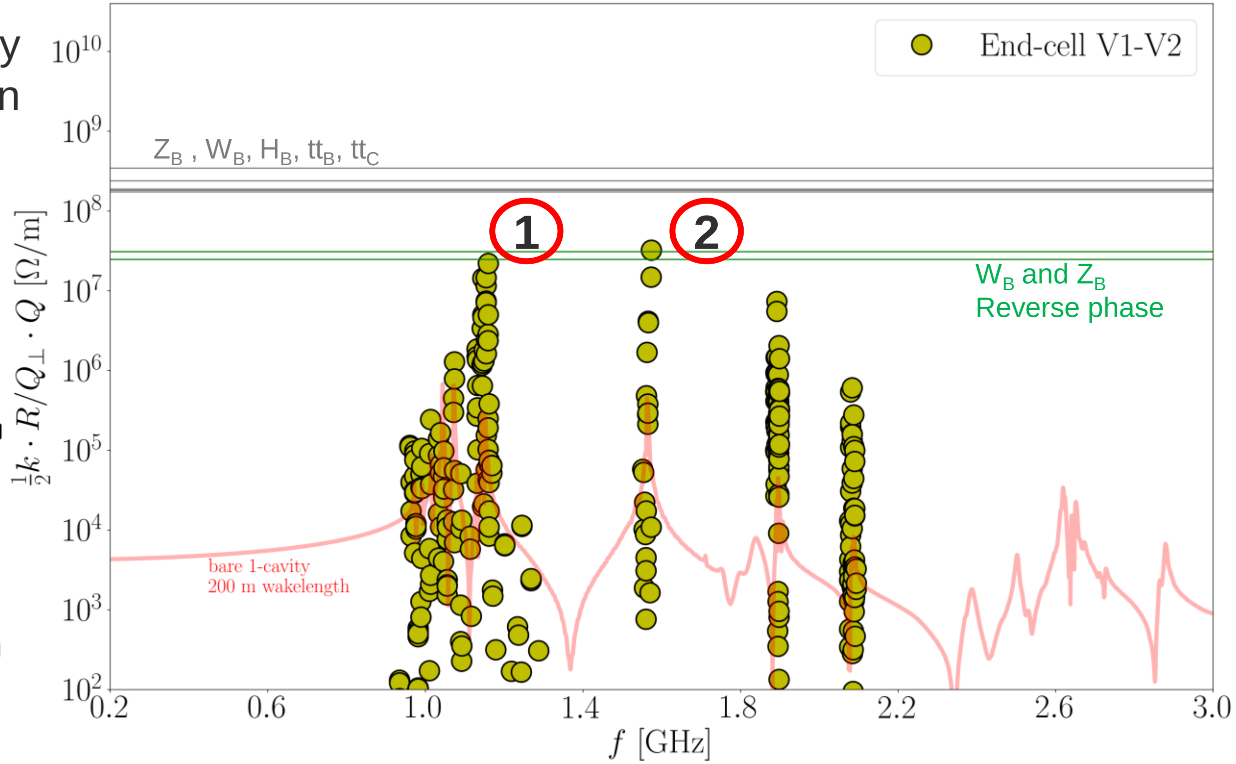

MP in DQW coupler

- Strong multipacting (MP) can occur in the DQW coupler at low E_{acc} (below 2 MV/m). Redesigning the shape of the capacitive section can help to eliminate MP in this coupler → to be studied

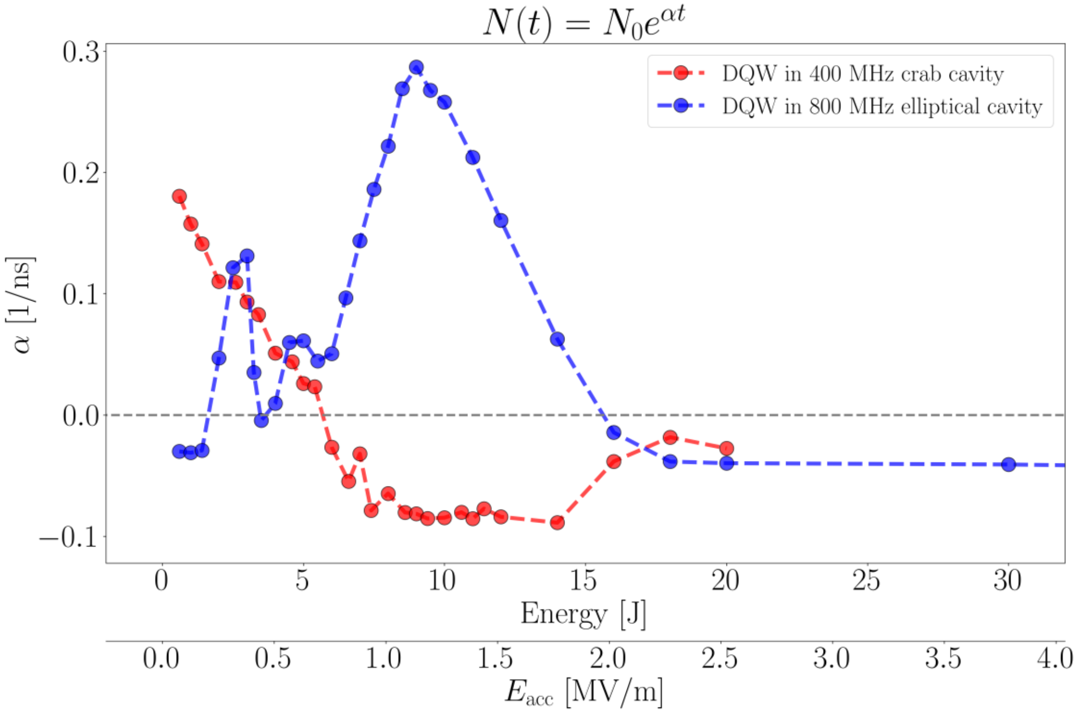

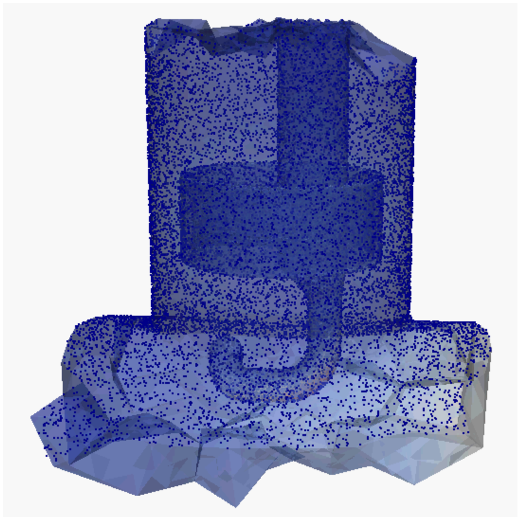

800 MHz elliptical cavity at 9 J in the cavity

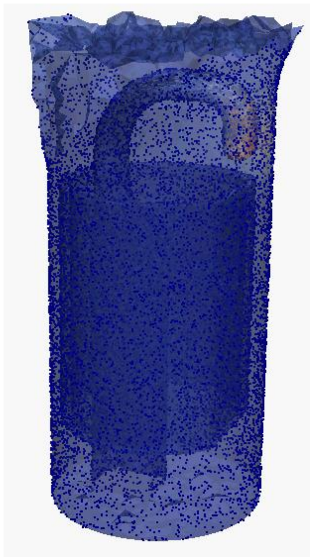

400 MHz crab cavity at 2 J in the cavity

Conclusion

- **Module Length reduction:**
  - Inner coaxial couplers removed; rely on BLA and additional empty ports for HOM damping
  - Saves ~0.8 m per module, potentially more with optimized tapering and BLA connections. Available vacuum gate valve diameter must be determined for further improvements!
- **Lower beam impedance limit at injection energy in RPO addressed by:**
  - Asymmetrical end-cell shape for better HOM damping
  - The other two HOM ports were used by a different HOM coupler design to cover modes at other passbands
  - Larger coupler dimensions for better mechanical robustness and inner cooling
  - Cell-sorting during manufacturing to minimize trapped HOMs
  - Stability achieved with limited margin
- **With the 6-cell cavity shape, port positions, and distances now fixed, these studies should follow:**
  - Improve HOM coupler designs for better HOM damping and reduced MP
  - Beam tracking in the booster cavities to better understand the beam stability limits

Appendix

Coupler kick calculation

- **Transverse Kick:** Each coupler imparts a transverse momentum kick Δp_x (or Δp_y) to the particle, causing a transverse deflection

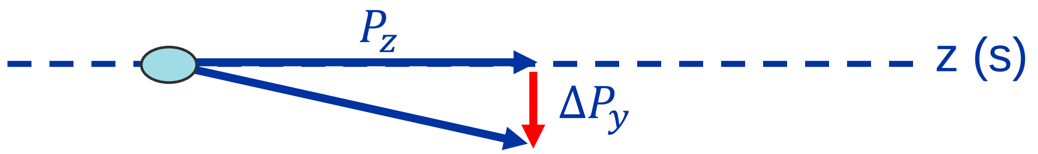

$$y' = \frac{dy}{ds} = \frac{\Delta P_y}{P_z} = \frac{\int F_y dt}{E/c} = \frac{q/c \int (E_y + c \times B_x) dz}{E/c} = \frac{qV_y}{E}$$

- **Drift between Cavities:** Between cavities, the particle drifts over a distance L. During this drift, its transverse position changes due to the momentum imparted by the previous kicks

$$\begin{bmatrix} y \\ y' \end{bmatrix} = \begin{bmatrix} 1 & R_{12} = L \\ 0 & 1 \end{bmatrix} \begin{bmatrix} y \\ y' \end{bmatrix} \quad \Longrightarrow \quad \Delta y = L\frac{qV_y}{E} = Lk$$

- **Net Effect of Multiple Cavities:** Over N cavities each with length L, the kicks add up in a cumulative manner, depending on the phase at which the particle encounters each kick. Assuming a constant transverse kick k from each coupler, independent of the particle's position across cavities, we have

$$y_N = y0 + NLk + (N-1)Lk + \cdots + 2Lk + Lk = y_0 + \frac{N(N+1)}{2}Lk$$

G. Burt, Transverse deflecting cavities

Coupler kick at 800 MHz

- To limit the kick offset caused by the couplers to below 1 mm (an arbitrary threshold to be determined based on beam dynamics and operational tolerances) in the booster cavities, corrector magnets are needed at least every 30 cavities (approximately 90 m) to steer the bunch back to the centre

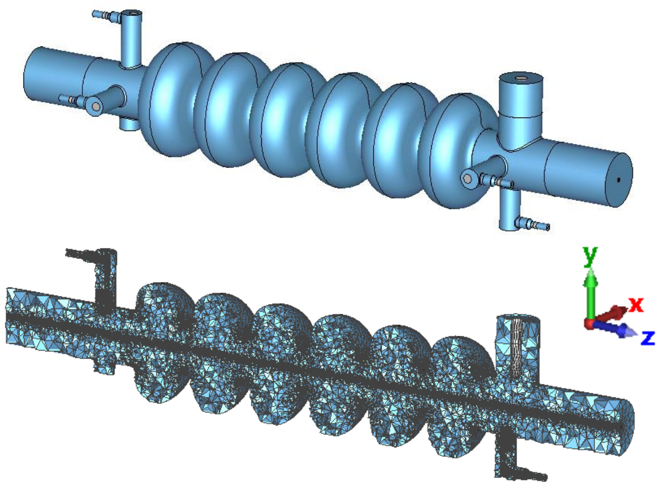

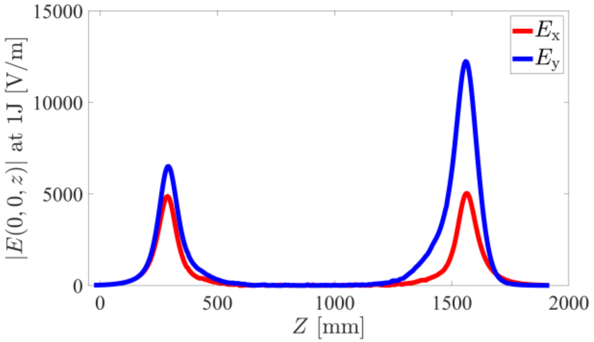

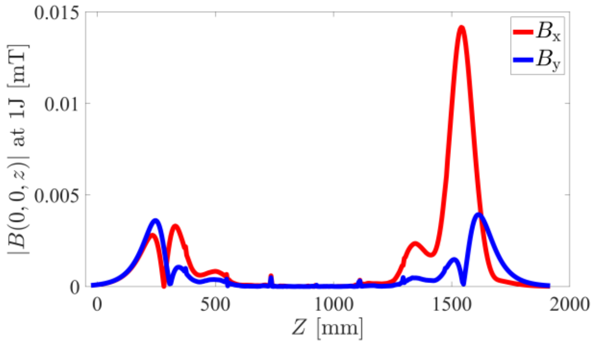

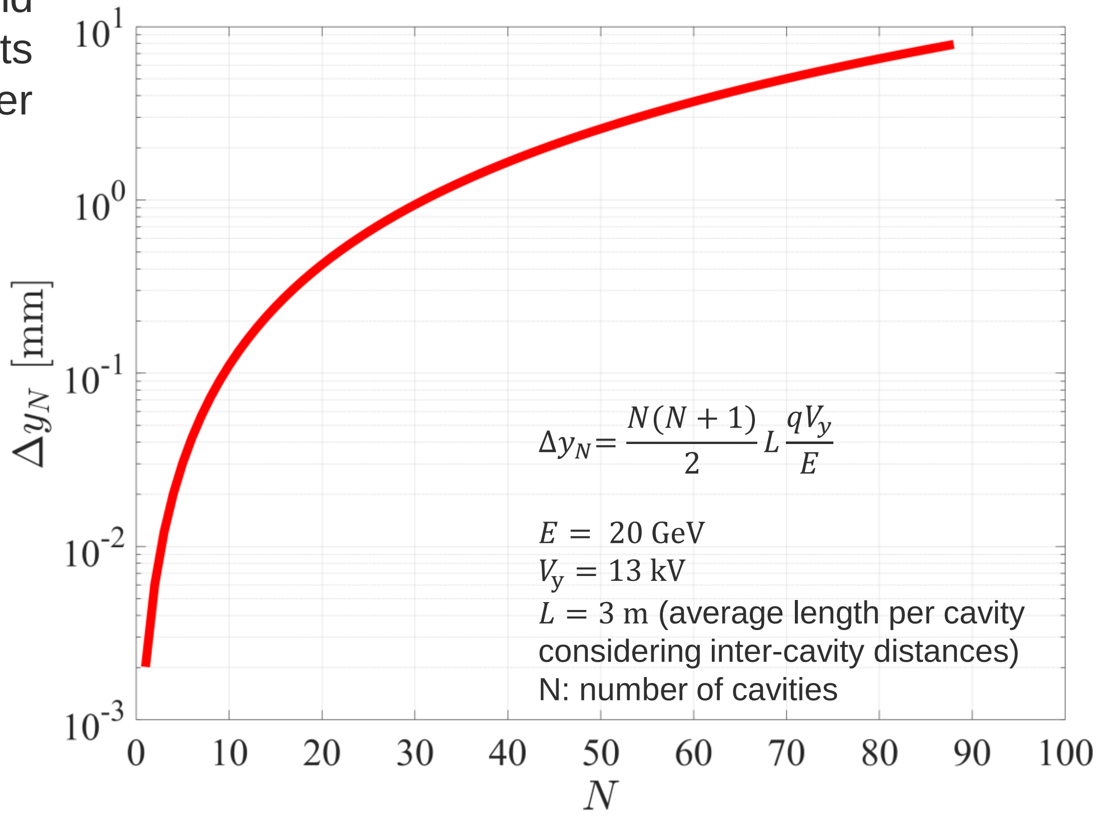

Convergence study of perturbation analysis

Mode 4 at FM passband

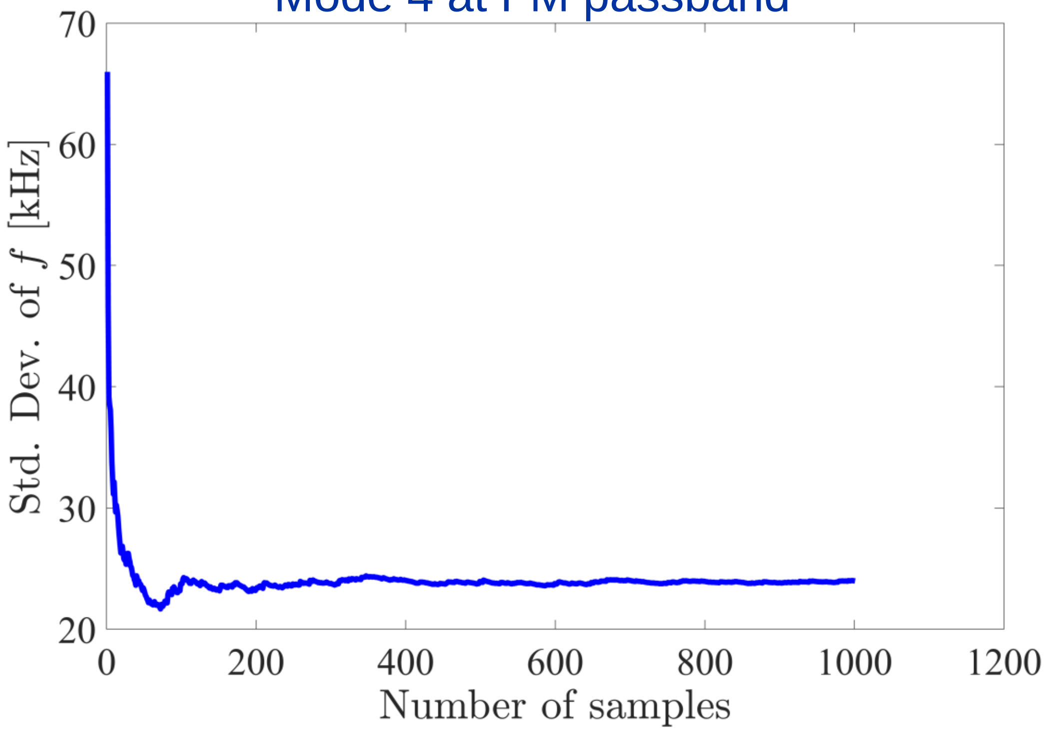

HM2

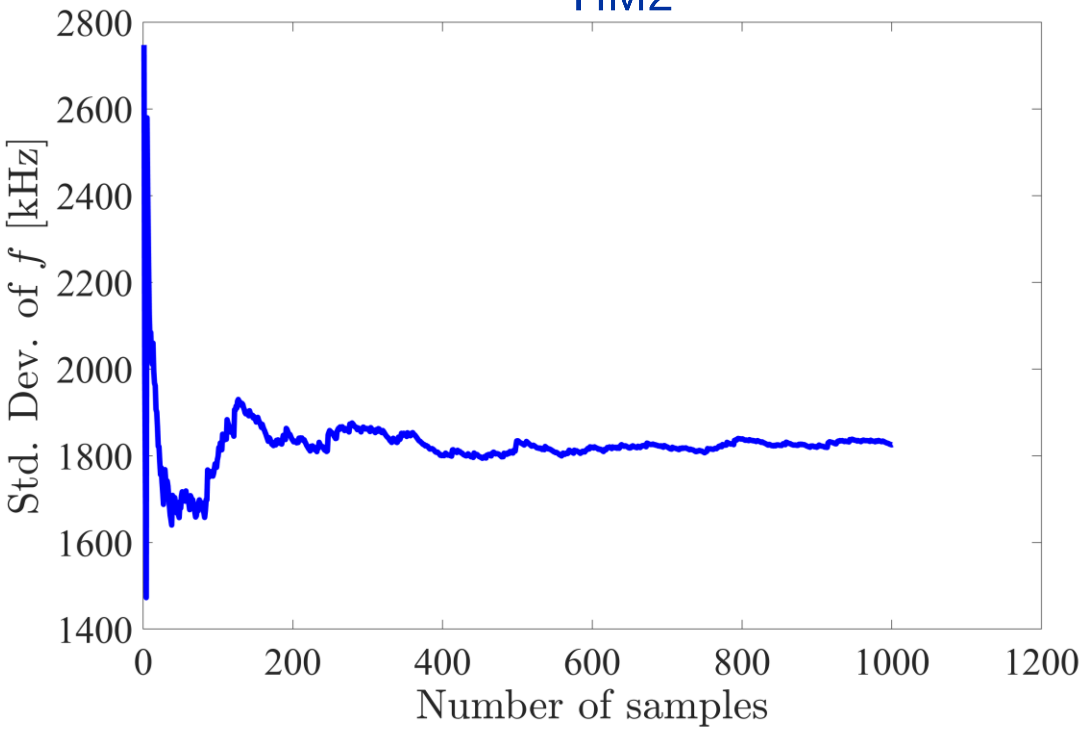

Cavity parameters

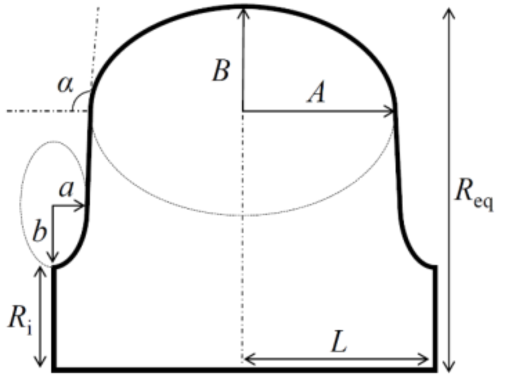

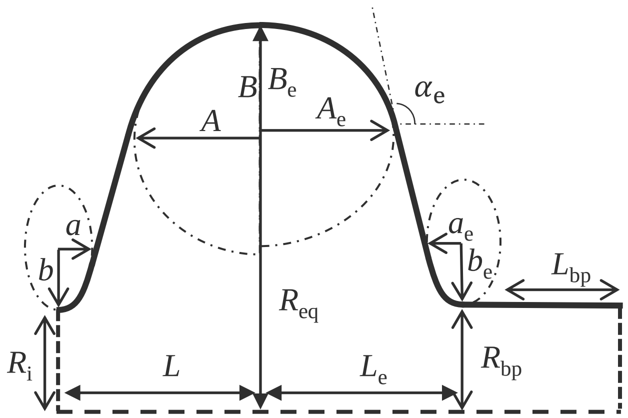

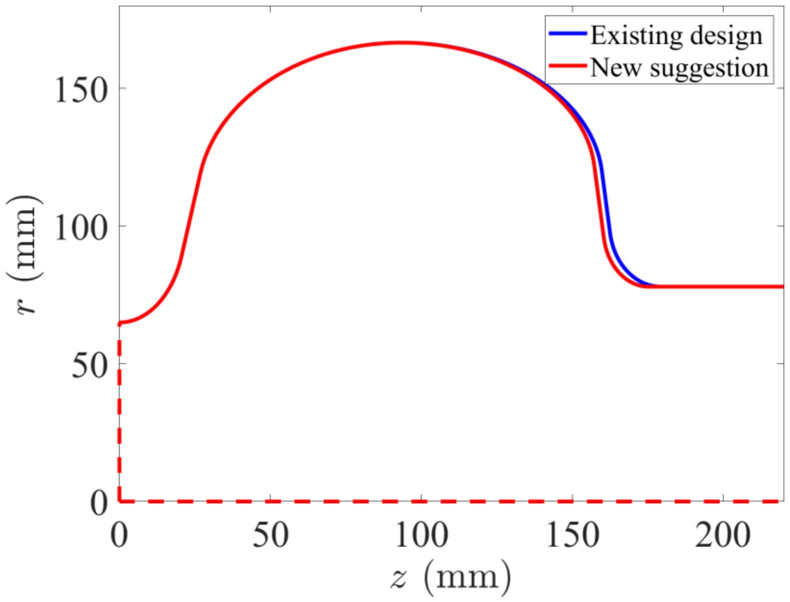

	A/A_e [mm]	B/B_e [mm]	a/a_e [mm]	b/b_e [mm]	R_i/R_{bp} [mm]	L/L_e [mm]	R_{eq} [mm]	α/α_e [°]
V1 End-cell	67.72/66.5	57.45/51.0	21.75/17.0	35.6/23.0	60.0/78.0	93.5/85.77	166.591	100.0/96.9
V2 End-cell	67.72/64	57.45/49	21.75/15	35.6/21	60.0/78.0	93.5/81.727	166.591	100.0/96.9

Mode at 2.367 GHz untrapping

- All analyzed end-cells have a radius of 78 mm, which is equal with the radius of the current design
- Among the geometries that satisfy the conditions $E_{\mathrm{pk}}/E_{\mathrm{acc}} < 2.1$, $B_{\mathrm{pk}}/E_{\mathrm{acc}} < 4.4\ \mathrm{mT/MV/m}$, and a wall angle of the end cell above 96 degrees, the one with the lowest TMI is selected

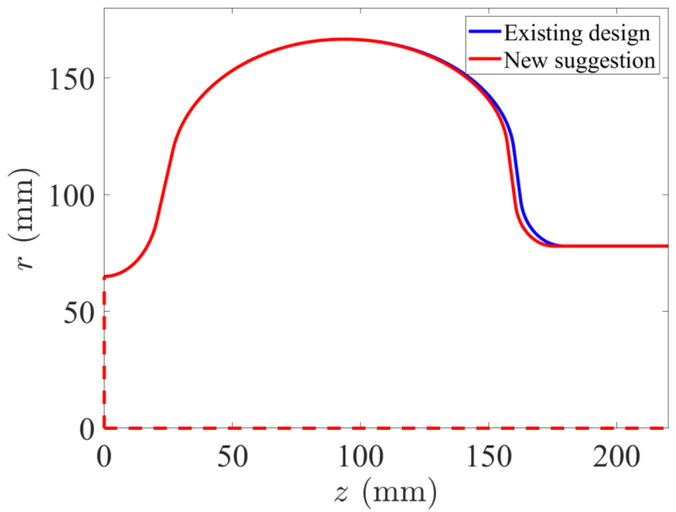

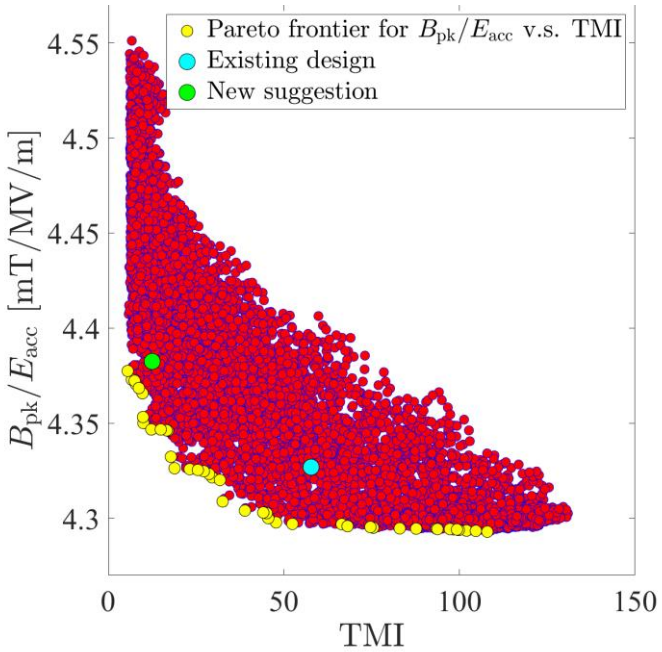

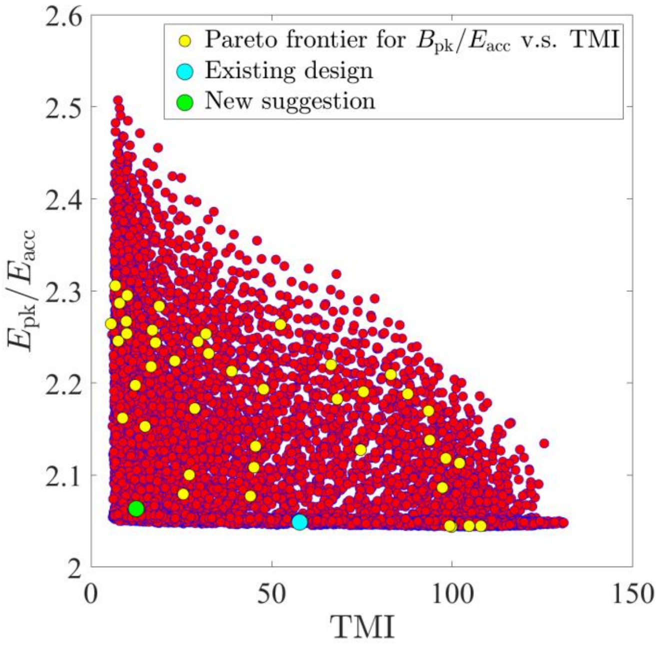

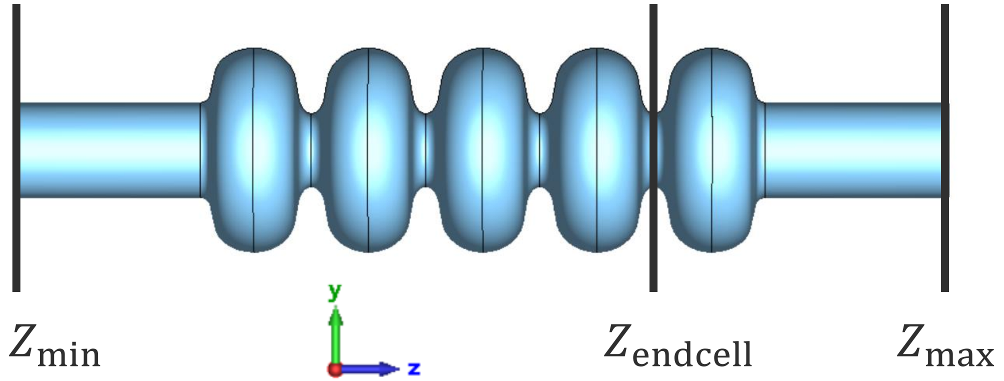

$$\text{Trapped mode index (TMI)} = \frac{\int_{Z_{\mathrm{min}}}^{Z_{\mathrm{max}}} \left|E_{(0,0,z)}\right|^2 \mathrm{d}z}{\int_{Z_{\mathrm{endcell}}}^{Z_{\mathrm{max}}} \left|E_{(0,0,z)}\right|^2 \mathrm{d}z}$$

New end-cell suggestion

Parameters	Existing end-cell design	New suggested end-cell
FM		
Frequency [MHz]	801.58	801.58
R/Q [Ω]	520.3	521.8
Geometry Factor [Ω]	272.9	271.6
$G.R/Q$ [kΩ²]	142.2	141.7
B_{pk}/E_{acc} [mT/(MV/m)]	4.33	4.38
E_{pk}/E_{acc} [-]	2.05	2.06
Cavity Active Length [mm]	919.532	911.454
Beam Pipe radius [mm]	78	78
Wall angle [degree]	100/96.9	100/96.9
Field Flatness [%]	99	99
HOM – Monopole modes		
Q_{ext} of mode f=1.494 GHz	3.5e3	2.2e3
Q_{ext} of mode f=2.367 GHz	4.5e3	1.5e3
Q_{ext} of mode f=3.38 GHz	8.0e3	3.7e3

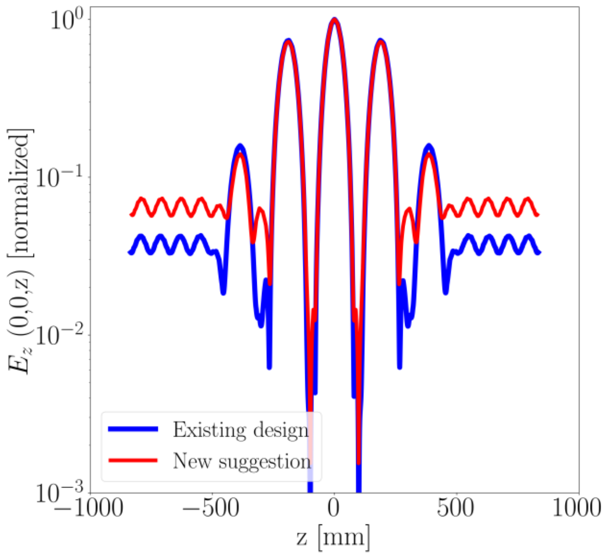

Mode at 2.367 GHz

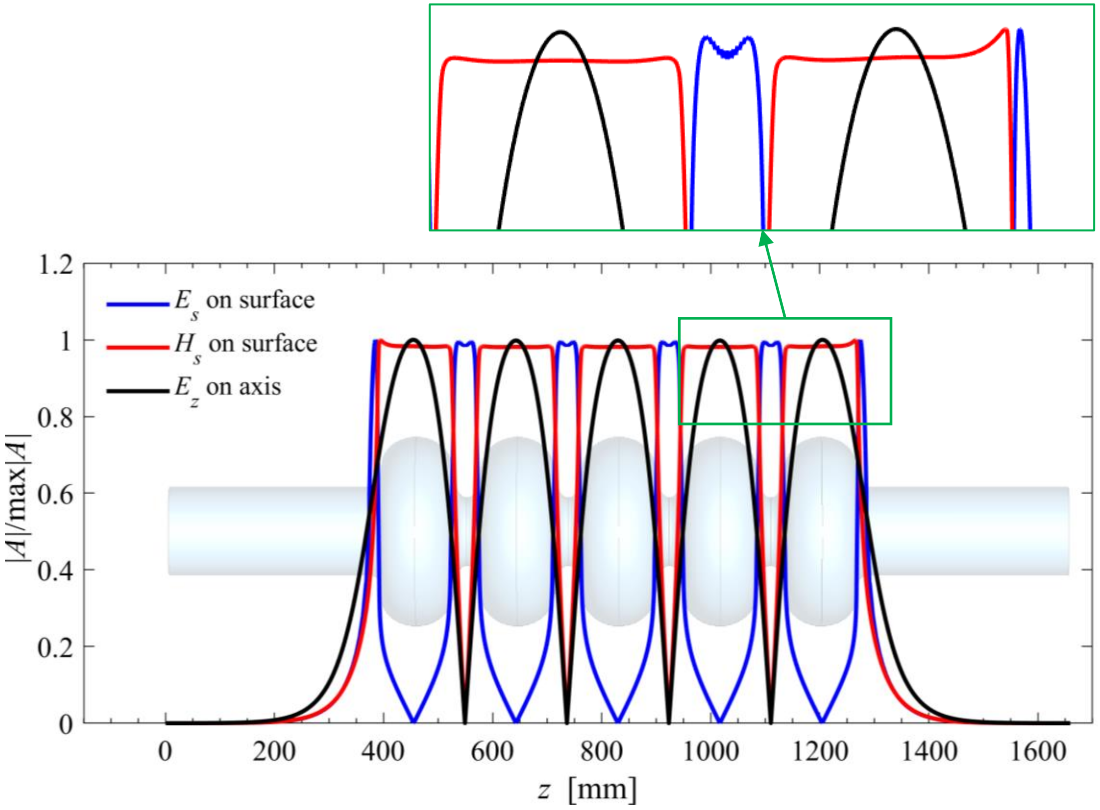

Fundamental mode

Impedance of the HOM damped cavity

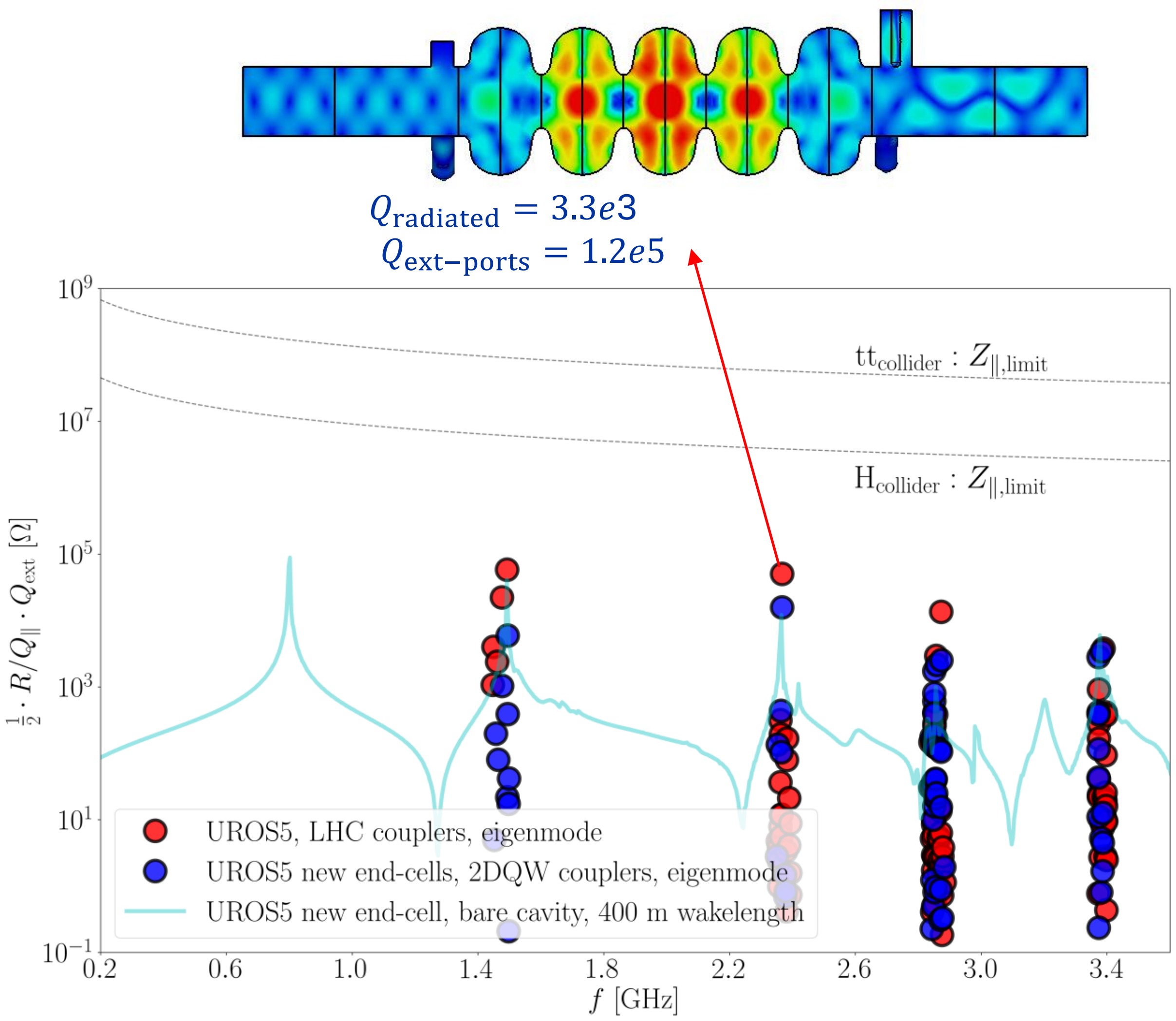

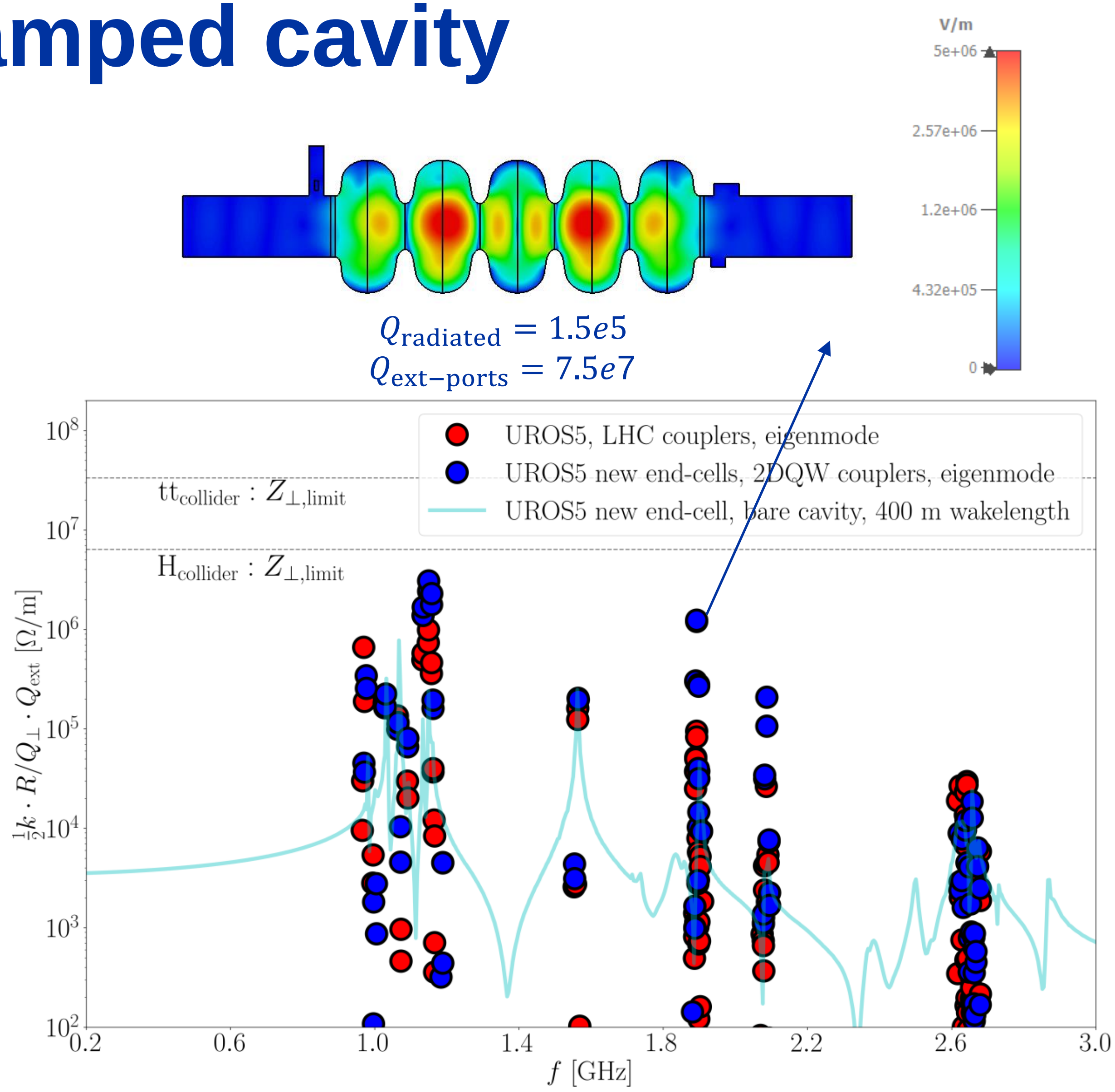

FM parameters of the 6-cell with asymmetric end-cells

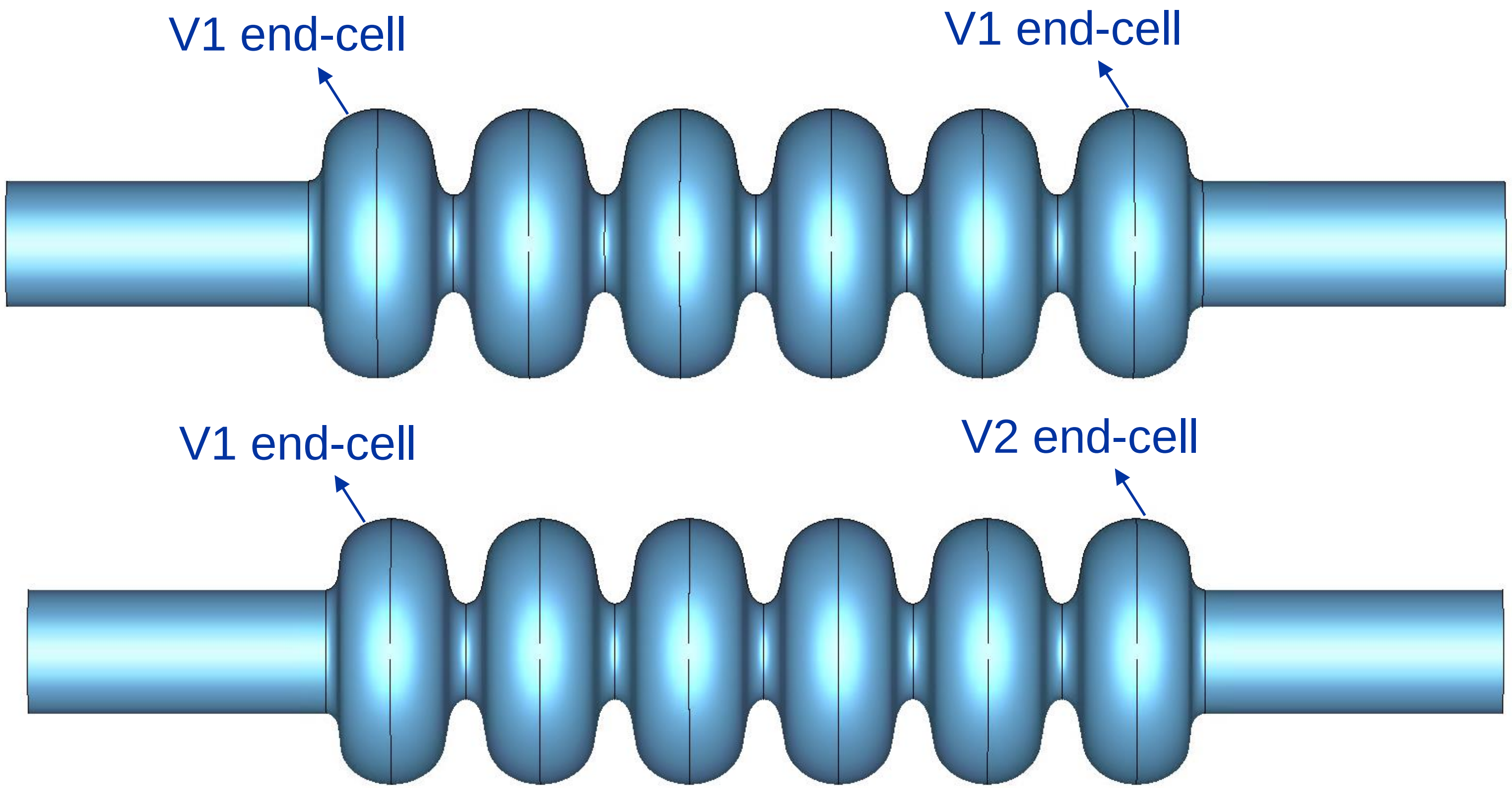

Parameters	V1 end-cell	V1-V2 end-cell
FM		
Frequency [MHz]	801.584	801.584
R/Q **[Ω]**	630.4	631.2
Geometry Factor [Ω]	272.8	272.2
$G.R/Q$ **[kΩ²]**	172.0	171.8
B_{pk}/E_{acc} [mT/(MV/m)]	4.31	**4.37**
E_{pk}/E_{acc} **[-]**	2.04	2.06
Cavity Active Length [mm]	1106.54	1102.497
Beam Pipe radius [mm]	78	78
Wall angle [degree]	100/96.9	100/96.9
Field Flatness [%]	99	99
HOM – Monopole modes		
Q_{ext} **of mode f=1.494 GHz**	5.0e3	**3.8e3**
Q_{ext} **of mode f=2.368 GHz**	9.0e3	**4.9e3**
Q_{ext} **of mode f=3.38 GHz**	1.0e4	**8.2e3**

FM passband sensitivity to perturbations for asymmetric end-cell

	m1	m2	m3	m4	m5	M6=FM	HM1	HM2	HM3
$\bar{f}$ [MHz]	784.929	788.100	792.556	797.048	800.358	801.581	-	2367.3	-
Std (f) [kHz]	84.5	67.7	46.8	23.7	8.8	3.2	-	2024	-
$\overline{R/Q}$ [Ω]	0.005	0.15	0.006	0.40	0.076	630.0	-	16.0	-
Q_{ext}	3.3e7	8.6e6	4.3e6	2.9e6	2.3e6	4.3e6	-	-	-
Q_{ext}	9.5e7	2.4e7	1.1e7	7.1e6	5.7e6	1.1e7	-	-	-

- $\bar{f}$ =mean value of frequency, and Std (f)=standard deviation of frequency
- HM is the higher order modes at different passbands with largest longitudinal R/Q
- 250 samples were taken